

Background-Free Near-Infrared Biphoton Emission from Single GaAs Nanowires

Grégoire Saerens,* Thomas Dursap, Ian Hesner, Ngoc M. H. Duong, Alexander S. Solntsev, Andrea Morandi, Andreas Maeder, Artemios Karvounis, Philippe Regreny, Robert J. Chapman, Alexandre Danescu, Nicolas Chauvin, José Penuelas, and Rachel Grange



Cite This: *Nano Lett.* 2023, 23, 3245–3250



Read Online

ACCESS |

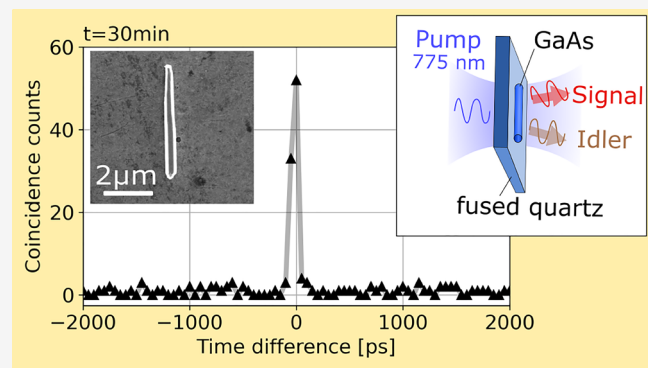
Metrics & More

Article Recommendations

Supporting Information

ABSTRACT: The generation of photon pairs from nanoscale structures with high rates is still a challenge for the integration of quantum devices, as it suffers from parasitic signals from the substrate. In this work, we report type-0 spontaneous parametric down-conversion at 1550 nm from individual bottom-up grown zinc-blende GaAs nanowires with lengths of up to 5 μm and diameters of up to 450 nm. The nanowires were deposited on a transparent ITO substrate, and we measured a background-free coincidence rate of 0.05 Hz in a Hanbury–Brown–Twiss setup. Taking into account transmission losses, the pump fluence, and the nanowire volume, we achieved a biphoton generation of 60 GHz/Wm, which is at least 3 times higher than that of previously reported single nonlinear micro- and nanostructures. We also studied the correlations between the second-harmonic generation and the spontaneous parametric down-conversion intensities with respect to the pump polarization and in different individual nanowires.

KEYWORDS: spontaneous parametric down-conversion, second-harmonic generation, III–V semiconductors, GaAs nanowires, room temperature



Miniaturization of biphoton light sources is an important requirement to achieve scalable and stable integrated quantum devices.¹ Photon pairs, or similarly heralded single photons, generated via spontaneous parametric down-conversion (SPDC) profit from high indistinguishability, room-temperature operation, simple signal filtering, and coherent emission as well as entanglement in several degrees of freedom.^{2–4} Applications have been demonstrated in different quantum technologies, including communication,^{5–10} imaging,^{11–13} computing,^{14–16} and metrology.^{17–19} Despite its intrinsically limited efficiency to avoid multiphoton events, compared, for example, to quantum dot- or atom-based photon sources,^{20,21} the brightness of SPDC-based photon sources can be improved with multiplexing without an increase in unwanted double-photon pairs.^{1,22,23}

Today's leading nonlinear light sources are bulk birefringent or periodically poled crystals^{24–26} and periodically poled waveguides,^{27–30} with millimeter length scales, for which phase matching is required. Miniaturization to the micrometer or submicrometer scale, to sizes smaller than the coherence length, relaxes the phase-matching condition and reduces the footprint of the source.³¹ SPDC with no phase-matching requirements has recently been demonstrated in thin

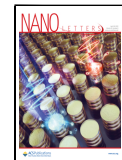
films^{32–34} and metasurfaces,^{35–38} for example by taking advantage of resonances such as bound states in the continuum or Mie resonances. A single nanoantenna does not need phase matching either,³⁹ and arrays of nanoantennas can be collectively excited for an increased generation rate. To our knowledge, SPDC generation from a single structure has only been demonstrated at 1550 nm in two different types of geometries, top-down AlGaAs nanoresonators⁴⁰ and free-standing LiNbO₃ microcubes.⁴¹ However, this has not been demonstrated in GaAs nanostructures despite the strong $\chi^{(2)}$ tensor ($d_{36} = 370 \text{ pm/V}^{42}$), high refractive index (3.4 for λ around 1550 nm⁴³), and various fabrication methods.

Here we report type-0 SPDC in individual self-assisted grown zinc-blende (ZB) GaAs nanowires (NWs) with lengths of $5.2 \pm 0.4 \mu\text{m}$ and diameters of $430 \pm 30 \text{ nm}$. Due to the

Received: January 3, 2023

Revised: April 12, 2023

Published: April 14, 2023



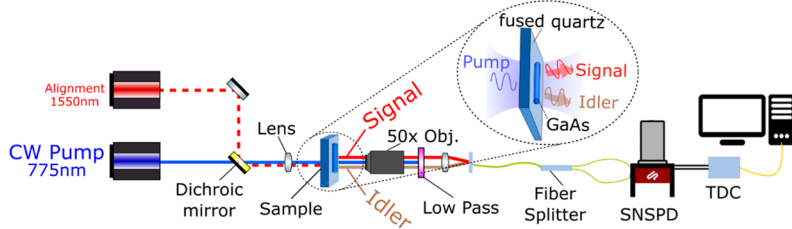


Figure 1. Hanbury–Brown–Twiss (HBT) setup using a continuous-wave pump laser with a wavelength of 775 nm. The photon pairs are collected with a 50 \times objective and filtered with two low-pass filters. Photons are detected with superconducting nanowire single-photon detectors (SNSPDs), and the coincidence counts of two channels are measured using a time-to-digital converter (TDC). The transmission in the fiber and the detection efficiency are both maximized using a 1550 nm laser.

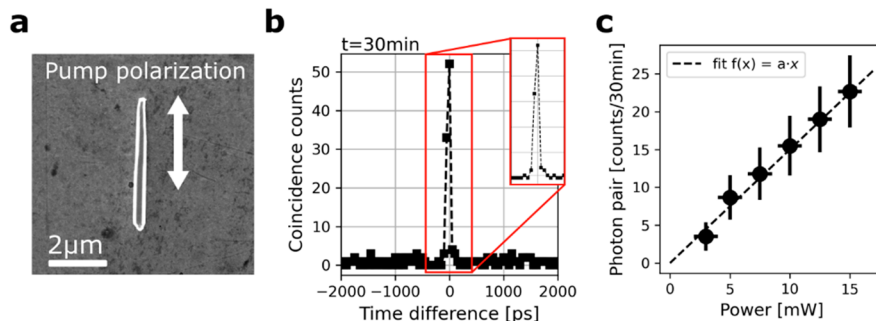


Figure 2. (a) Scanning electron microscopy (SEM) image of the GaAs nanowire (NW) with a length of 5 μm and a diameter of 450 nm. The linear polarization of the pump, which is along the long axis of the NW, is indicated by the white arrow. (b) Coincidence counts measured over 30 min with a maximum count of 52 at zero-time difference and a coincidences-to-accidentals ratio (CAR) well above 2. The detected biphoton arrivals is calculated as the sum of the coincidence counts around zero-time difference, which is 90 here. (c) Linear dependence of photon-pair counts with incoming pump power.

high tensor components of the GaAs crystal structure compared to other typical nonlinear materials (β -barium borate, potassium dihydrogen phosphate, or lithium niobate), and the possibility to place the NW on a transparent substrate, we obtained at room temperature and for 15 mW incident power a high photon-pair rate of 0.05 Hz with a corresponding coincidences-to-accidentals ratio (CAR) of 60 in the coincidence histogram. The efficiency given as a transmission-corrected photon pair rate normalized to the excitation fluence and nanostructure volume was 60 GHz/Wm. This is 40 times higher than that of AlGaAs nanoresonator⁴⁰ and 3 times higher than that of LiNbO₃ microcube systems.⁴¹

Self-assisted GaAs NWs with a ZB crystal structure and a slight Be p-doping were grown by molecular beam epitaxy on a silicon (111) substrate. It should be noted that the NWs also possess a short defective region at the bottom and at the top, including a wurtzite (WZ) segment at the top.⁴⁴ After growth, the NWs were mechanically transferred to a transparent thin ITO layer (10 nm) on an SiO₂ substrate. The detailed fabrication steps are given in section 1 of the Supporting Information. In section 2 of the Supporting Information, we characterized the NWs optically. We show on the one hand that the NWs are nonresonant around 775 and 1550 nm by collecting the scattering spectrum using a dark field microscope. On the other hand, we confirm optically the crystal uniformity in the middle of the NWs by imaging the dependence of the second-harmonic-generation (SHG) intensity with the linear polarization of the incoming pump laser.⁴⁵ We recorded SPDC with a Hanbury–Brown–Twiss (HBT) setup as shown in Figure 1. First, a linearly polarized

continuous-wave laser with a wavelength of 775 nm and 15 mW power was focused with a lens ($f = 8$ mm) on a single NW. The generated photon pairs were then collected with a 50 \times NIR objective ($f = 4$ mm) and separated from the pump with two low-pass filters. After that, the light was coupled to a 1550 nm fiber, split in two channels, and finally detected with superconducting nanowire single-photon detectors (SNSPDs). A time-to-digital converter (TDC) was used to measure coincidence counts between the two channels. A 1550 nm laser was used for the SHG process and to maximize the fiber transmission and detection efficiency. In section 3 of the Supporting Information, we describe the setup in detail and give the alignment procedure to measure photon pairs. We discuss in section 4 of the Supporting Information the impact of the pump wavelength, which is smaller than the band gap of GaAs.

We excite a GaAs NW with a length of 5 μm and a diameter of 450 nm using a linearly polarized laser along its crystal axis, with a spot size of around 6 μm radius (Figure 2a). The measured coincidence counts over 30 min show a photon pair rate of 0.05 Hz (90 counts over 30 min, see Figure 2b) with a CAR equal to 60, which should be greater than 2 for photon pairs. The accidental counts are much lower than the signal counts because the NW is lying on a transparent substrate. The SPDC process is also confirmed by the linear increase in photon pairs with respect to the incoming power, as shown in Figure 2c, indicating that only one photon is involved as a pump in the nonlinear process. Phase matching in such nanostructures is not necessary, as the coherence length of GaAs is around 2.7 μm , which is much more than the thickness

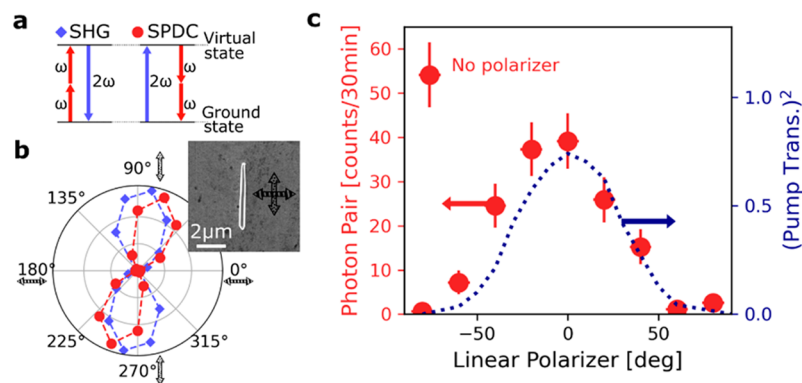


Figure 3. (a) Schematic of energy transitions involved in the SHG and SPDC process. (b) Normalized SHG (blue diamonds) and SPDC (red circles) signal for different linear polarization orientations of the pump. The inset shows the same SEM image of the NW as in Figure 2a. The lighter (darker) arrow corresponds to pump photons linearly polarized at 90°/270° (0°/180°) with respect to the horizon (laboratory reference frame). (c) Similar measurement at a fixed pump polarization (90°/270°) with a linear polarizer set before the fiber in-coupling. We give with red dots the photon pairs measured for different orientations of the polarizer and with the blue dotted line the expected squared transmission from photons polarized along the NW's axis, as the 775 nm pump laser.

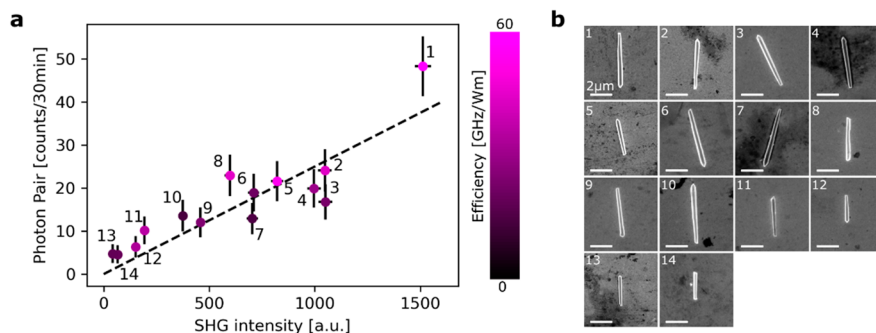


Figure 4. (a) Correlation between SHG (*x*-axis) and SPDC (*y*-axis) intensity for 14 different NWs. The measured biphoton rates normalized to the transmission losses, volume, and (fixed) pump fluence are given as efficiencies with the pink scale bar. The maximum calculated efficiency was 60 GHz/Wm. (b) SEM images of the 14 single NWs.

of the NW (see calculation in section 4 of the Supporting Information).

From the quantum-classical correspondence relation between SPDC and SHG as depicted in Figure 3a,⁴⁶ we expected a similar polarization dependence of the second-order nonlinear signals for nonresonant structures,⁴¹ and we could indeed observe it. The SPDC (SHG) intensity measured for different polarizations of the 775 nm (1550 nm) pump laser is indicated by red circles (blue diamonds) in Figure 3b. A maximum SPDC (SHG) signal intensity was obtained for a linear polarization along the NW. In addition, we characterized the polarization of the photon pairs by placing a linear polarizer before the fiber coupling. The linear polarization of the pump was fixed along the NW, for which the photon-pair rate without polarizer was the highest, as shown previously in Figure 2b. Figure 3c shows in red the photon pair counts without a polarizer and for different orientations of the polarizer. We measured a maximum photon-pair rate for the polarizer oriented along the NW and no signal for the polarizer oriented perpendicularly to the NW. As a matter of fact, the maximum rate was only (90%)² of that of the biphoton rate without polarizer, which corresponds to the transmission losses of photon pairs from the polarizer. We compared the impact of the polarizer's rotation on the photon-pair rate (red points) directly with the transmission squared of a 1550 nm laser (blue curve), for which the linear polarization was the same as the SPDC pump laser. We observed a very good matching; as

shown in Figure 3c, the NW emits photon pairs with the same polarization as the excitation light, along the NW's axis. We thus conclude that the SPDC is type-0 for NWs pumped along the long axis. Similar polarization-dependent Raman scattering, SHG, or single-photon emission have already been observed from single NWs.^{45,47–50} Considering the crystal structure orientation of our GaAs NWs, in our case, the dependence of SHG and SPDC on the pump polarization matched the expectation from our calculation of the $\chi^{(2,i)}$ tensor in the rotation frame $i = 1, 2, 3$. In section 5 of the Supporting Information we show similar polarization-dependent SHG emission profiles for 14 different NWs. The $\chi_{x,x,x}^{(2)}$ value leads indeed to a strong SHG emission intensity for x -polarization, which is along the NW's axis. The slight mismatch between the polarization measurement shown in Figure 3b,c can be understood from the alignment procedure, which involves multiple waveplates (see section 3 in the Supporting Information).

Finally, we measured similarly the second-order nonlinear intensities (SHG and SPDC) from 14 single GaAs NWs. We observed a linear correlation between SHG intensity and biphoton rates, as shown in Figure 4. NWs generating low SHG intensities also emit low photon-pair rates. We noticed that the nonlinear emission intensity did not depend on the NW's size: see for example NW no. 10 in Figure 4 with a higher volume compared to the average but with lower nonlinear intensities. We confirmed this dependence by

analyzing more in detail the impact of the NW's size on the biphoton rate (see section 6 of the Supporting Information). We also evaluated for each NW if their linear optical properties were correlated with the nonlinear emission. We found for each NW that the linear optical properties are not strongly correlated with the nonlinear emission. When taking into account the losses in the setup (objective transmission, fiber in-coupling, fiber splitter, and detector), we find a photon-pair rate of up to 20 Hz. This correction does not take into account photon pairs emitted backward or forward but only collected by a NA = 0.65 objective. In order to compare with other miniaturized sources, we normalized this transmission-corrected rate as in Marino et al.⁴⁰ with the volume of the NW and the pump fluence. The resulting efficiency of the SPDC process can reach 60 GHz/Wm for GaAs NWs (see purple scale bar in Figure 4a). The detailed calculations and the numerical values of the efficiencies are given in section 6 of the Supporting Information. The overall crystal structure uniformity is shown in Figures S3 and S4 of the Supporting Information, but nanoscopic crystal structure defects or doping concentration variations may be present and could still have some impact on the biphoton emission efficiency. In comparison, the SPDC efficiency from GaAs NWs is 40 times higher than that of similar AlGaAs nanoantennas⁴⁰ and 3 times higher than that of LiNbO₃ microcubes.⁴¹ We consider this was possible thanks to the NW's growth and transfer method and the geometry of the system, the one-dimensionality of the NW, leading to an accessible and strong d_{36} component of the bulk GaAs ZB $\chi^{(2)}$ tensor.

CONCLUSION

We have investigated type-0 photon pairs generated at 1550 nm wavelength from SPDC in single GaAs NWs. We have tested the quantum-classical correspondence by comparing on the one hand the pump polarization impact on the SHG intensity with the SPDC rate and on the other hand the nonlinear generation from 14 similar NWs. We observed a linear correlation between SPDC and SHG intensities. For individual self-assisted grown ZB GaAs NWs with 5 μm length and 450 nm diameter we obtained a maximum photon pair rate of 20 Hz. We have demonstrated GaAs NWs as photon pair sources profiting from stability, time coherence, and room-temperature operation. These structures could be directly grown on a photonic chip or transferred and freely positioned on it using an atomic force microscopy tip. They would act as quantum light emitters that do not need quantum confinement engineering. Further study into the geometry and crystal orientation of III–V nanostructures would benefit research not only in nonlinear processes such as SHG and SPDC but also in single-photon emitters such as defects and quantum dots.

ASSOCIATED CONTENT

Supporting Information

The Supporting Information is available free of charge at <https://pubs.acs.org/doi/10.1021/acs.nanolett.3c00026>.

Details of fabrication, nanowire optical characterization, setup, and alignment to measure SHG and SPDC, the GaAs coherence length, the GaAs bulk $\chi^{(2)}$ tensor specific to this experiment, and a summary of the NW efficiency (PDF)

AUTHOR INFORMATION

Corresponding Author

Grégoire Saerens – ETH Zurich, Department of Physics, Institute for Quantum Electronics, Optical Nanomaterial Group, 8093 Zurich, Switzerland;  orcid.org/0000-0001-8568-8462; Email: gsaerens@phys.ethz.ch

Authors

Thomas Dursap – Univ. Lyon, CNRS, ECL, INSA Lyon, UCBL, CPE Lyon, INL, UMR 5270, 69130 Ecully, France

Ian Hesner – ETH Zurich, Department of Physics, Institute for Quantum Electronics, Optical Nanomaterial Group, 8093 Zurich, Switzerland

Ngoc M. H. Duong – ETH Zurich, Department of Physics, Institute for Quantum Electronics, Optical Nanomaterial Group, 8093 Zurich, Switzerland;  orcid.org/0000-0002-1149-6342

Alexander S. Solntsev – University of Technology Sydney, School of Mathematical and Physical Sciences, Ultimo, New South Wales 2007, Australia;  orcid.org/0000-0003-4981-9730

Andrea Morandi – ETH Zurich, Department of Physics, Institute for Quantum Electronics, Optical Nanomaterial Group, 8093 Zurich, Switzerland;  orcid.org/0000-0001-8199-1536

Andreas Maeder – ETH Zurich, Department of Physics, Institute for Quantum Electronics, Optical Nanomaterial Group, 8093 Zurich, Switzerland

Artemios Karvounis – ETH Zurich, Department of Physics, Institute for Quantum Electronics, Optical Nanomaterial Group, 8093 Zurich, Switzerland

Philippe Regreny – Univ. Lyon, CNRS, ECL, INSA Lyon, UCBL, CPE Lyon, INL, UMR 5270, 69130 Ecully, France

Robert J. Chapman – ETH Zurich, Department of Physics, Institute for Quantum Electronics, Optical Nanomaterial Group, 8093 Zurich, Switzerland;  orcid.org/0000-0002-0368-8483

Alexandre Danescu – Univ. Lyon, CNRS, ECL, INSA Lyon, UCBL, CPE Lyon, INL, UMR 5270, 69130 Ecully, France

Nicolas Chauvin – Univ. Lyon, CNRS, ECL, INSA Lyon, UCBL, CPE Lyon, INL, UMR 5270, 69130 Ecully, France

José Penuelas – Univ. Lyon, CNRS, ECL, INSA Lyon, UCBL, CPE Lyon, INL, UMR 5270, 69130 Ecully, France;  orcid.org/0000-0002-5635-7346

Rachel Grange – ETH Zurich, Department of Physics, Institute for Quantum Electronics, Optical Nanomaterial Group, 8093 Zurich, Switzerland;  orcid.org/0000-0001-7469-9756

Complete contact information is available at:

<https://pubs.acs.org/10.1021/acs.nanolett.3c00026>

Author Contributions

The manuscript was written through contributions of all authors. R.G., R.J.C., A.S.S., and G.S. designed the experiment. G.S., A. Maeder, and N.D. built the setup, and G.S. and I.H. conducted the experiments. T.D., P.R., A.D., N.C., and J.P. fabricated the GaAs NWs. A. Morandi and A.K. took the SEM images of the NWs. G.S., T.D., R.J.C., and R.G. wrote the manuscript. All authors have given approval to the final version of the manuscript.

Notes

The authors declare no competing financial interest.

ACKNOWLEDGMENTS

The authors thank the Scientific Centre for Optical and Electron Microscopy (ScopeM) of Eidgenössische Technische Hochschule (ETH) Zürich and the NanoLyon platform for access to equipment and J. B. Goure for technical assistance. This work was supported by the European Union's Horizon 2020 research and innovation program from the European Research Council under the Grant Agreement No. 714837 (Chi2-nano-oxides), the Australian Research Council DE180100070, and the French Agence Nationale de la Recherche (ANR) for funding (project BEEP ANR-18-CE05-0017-01).

ABBREVIATIONS

NWnanowire; SPDCspontaneous parametric down-conversion; SHGsecond-harmonic generation; ZBzinc-blende; CAR-coincidences-to-accidentals ratio; HBTHanbury–Brown–Twiss; SNSPDsuperconducting nanowire single-photon detector; TDCtime-to-digital converter

REFERENCES

- (1) Meyer-Scott, E.; Silberhorn, C.; Migdall, A. Single-Photon Sources: Approaching the Ideal through Multiplexing. *Rev. Sci. Instrum.* **2020**, *91* (4), 041101.
- (2) Meraner, S.; Chapman, R. J.; Frick, S.; Prilmüller, M.; Weihs, G.; et al. Approaching the Tsirelson Bound with a Sagnac Source of Polarization-Entangled Photons. *SciPost Phys.* **2021**, *10* (1), 1–18.
- (3) Brendel, J.; Gisin, N.; Tittel, W.; Zbinden, H. Pulsed Energy-Time Entangled Twin-Photon Source for Quantum Communication. *Phys. Rev. Lett.* **1999**, *82* (12), 2594.
- (4) Morrison, C. L.; Graffitti, F.; Barrow, P.; Pickston, A.; Ho, J.; Fedrizzi, A. Frequency-Bin Entanglement from Domain-Engineered down-Conversion. *APL Photonics* **2022**, *7* (6), 066102.
- (5) Burnham, D. C.; Weinberg, D. L. Observation of Simultaneity in Parametric Production of Optical Photon Pairs. *Phys. Rev. Lett.* **1970**, *25* (2), 84–87.
- (6) Bouwmeester, D.; Pan, J. W.; Mattle, K.; Eibl, M.; Weinfurter, H.; Zeilinger, A. Experimental Quantum Teleportation. *Nature* **1997**, *390*, 575–579.
- (7) Jennewein, T.; Simon, C.; Weihs, G.; Weinfurter, H.; Zeilinger, A. Quantum Cryptography with Entangled Photons. *Phys. Rev. Lett.* **2000**, *84* (20), 4729–4732.
- (8) Ursin, R.; Tiefenbacher, F.; Schmitt-Manderbach, T.; Weier, H.; Scheidl, T.; Lindenthal, M.; Blauensteiner, B.; Jennewein, T.; Perdigues, J.; Trojek, P.; et al. Entanglement-Based Quantum Communication over 144km. *Nat. Phys.* **2007**, *3* (7), 481–486.
- (9) Lo, H. K.; Curty, M.; Tamaki, K. Secure Quantum Key Distribution. *Nat. Photonics* **2014**, *8* (8), 595–604.
- (10) Wang, X. L.; Cai, X. D.; Su, Z. E.; Chen, M. C.; Wu, D.; Li, L.; Liu, N. Le; Lu, C. Y.; Pan, J. W. Quantum Teleportation of Multiple Degrees of Freedom of a Single Photon. *Nature* **2015**, *518* (7540), 516–519.
- (11) Pittman, T. B.; Shih, Y. H.; Strekalov, D. V.; Sergienko, A. V. Optical Imaging by Means of Two-Photon Quantum Entanglement. *Phys. Rev. A* **1995**, *52* (5), R3429–R3432.
- (12) Wolley, O.; Gregory, T.; Beer, S.; Higuchi, T.; Padgett, M. Quantum Imaging with a Photon Counting Camera. *Sci. Rep.* **2022**, *12* (1), 1–9.
- (13) Lugiato, L. A.; Gatti, A.; Brambilla, E. Quantum Imaging. *J. Opt. B Quantum Semiclass. Opt.* **2002**, *4*, S176–S183.
- (14) Pittman, T. B.; Fitch, M. J.; Jacobs, B. C.; Franson, J. D. Experimental Controlled-NOT Logic Gate for Single Photons in the Coincidence Basis. *Phys. Rev. A - At. Mol. Opt. Phys.* **2003**, *68* (3), 032316.
- (15) Zhong, H.-S.; Li, Y.; Li, W.; Peng, L. C.; Su, Z. E.; Hu, Y.; He, Y. M.; Ding, X.; Zhang, W.; Li, H.; et al. 12-Photon Entanglement and Scalable Scattershot Boson Sampling with Optimal Entangled-Photon Pairs from Parametric Down-Conversion. *Phys. Rev. Lett.* **2018**, *121* (25), 1–6.
- (16) Heitert, P.; Buldt, F.; Bassène, P.; N'Gom, M. Producing Multiple Qubits via Spontaneous Parametric Down-Conversion. *Phys. Rev. Appl.* **2021**, *16* (6), 064048.
- (17) Brida, G.; Genovese, M.; Gramegna, M.; Rastello, M. L.; Chekhova, M.; Krivitsky, L. Single-Photon Detector Calibration by Means of Conditional Polarization Rotation. *J. Opt. Soc. Am. B* **2005**, *22* (2), 488.
- (18) Castelletto, S.; Degiovanni, I. P.; Schettini, V.; Migdall, A. Optimizing Single-Photon-Source Heralding Efficiency and Detection Efficiency Metrology at 1550 nm Using Periodically Poled Lithium Niobate. *Metrologia* **2006**, *43* (2), S56.
- (19) Polino, E.; Valeri, M.; Spagnolo, N.; Sciarrino, F. Photonic Quantum Metrology. *AVS Quantum Sci.* **2020**, *2* (2), 024703.
- (20) Somaschi, N.; Giesz, V.; De Santis, L.; Loredo, J. C.; Almeida, M. P.; Hornecker, G.; Portalupi, S. L.; Grange, T.; Antón, C.; Demory, J.; et al. Near-Optimal Single-Photon Sources in the Solid State. *Nat. Photonics* **2016**, *10* (5), 340–345.
- (21) Jöns, K. D.; Schweikert, L.; Versteegh, M. A. M.; Dalacu, D.; Poole, P. J.; Gulinatti, A.; Giudice, A.; Zwiller, V.; Reimer, M. E. Bright Nanoscale Source of Deterministic Entangled Photon Pairs Violating Bell's Inequality. *Sci. Rep.* **2017**, *7* (1), 1–11.
- (22) Collins, M. J.; Xiong, C.; Rey, I. H.; Vo, T. D.; He, J.; Shahnia, S.; Reardon, C.; Krauss, T. F.; Steel, M. J.; Clark, A. S.; et al. Integrated Spatial Multiplexing of Heralded Single-Photon Sources. *Nat. Commun.* **2013**, *4* (1), 1–7.
- (23) Mower, J.; Englund, D. Efficient Generation of Single and Entangled Photons on a Silicon Photonic Integrated Chip. *Phys. Rev. A - At. Mol. Opt. Phys.* **2011**, *84* (5), 1–7.
- (24) Li, L.; Liu, Z.; Ren, X.; Wang, S.; Su, V. C.; Chen, M. K.; Chu, C. H.; Kuo, H. Y.; Liu, B.; Zang, W.; et al. Metalens-Array-Based High-Dimensional and Multiphoton Quantum Source. *Science* (80-). **2020**, *368* (6498), 1487–1490.
- (25) Kwiat, P. G.; Mattle, K.; Weinfurter, H.; Zeilinger, A.; Sergienko, A. V.; Shih, Y. New High-Intensity Source of Polarization-Entangled Photon Pairs. *Phys. Rev. Lett.* **1995**, *75* (24), 4337–4341.
- (26) Mair, A.; Vaziri, A.; Weihs, G.; Zeilinger, A. Entanglement of the Orbital Angular Momentum States of Photons. *Nature* **2001**, *412*, 313–316.
- (27) Kurimura, S.; Kato, Y.; Maruyama, M.; Usui, Y.; Nakajima, H. Quasi-Phase-Matched Adhered Ridge Waveguide in LiNbO₃. *Appl. Phys. Lett.* **2006**, *89* (19), 191123.
- (28) Xue, G. T.; Niu, Y. F.; Liu, X.; Duan, J. C.; Chen, W.; Pan, Y.; Jia, K.; Wang, X.; Liu, H. Y.; Zhang, Y.; et al. Ultrabright Multiplexed Energy-Time-Entangled Photon Generation from Lithium Niobate on Insulator Chip. *Phys. Rev. Appl.* **2021**, *15* (6), 1.
- (29) Zhao, J.; Ma, C.; Rüsing, M.; Mookherjea, S. High Quality Entangled Photon Pair Generation in Periodically Poled Thin-Film Lithium Niobate Waveguides. *Phys. Rev. Lett.* **2020**, *124* (16), 163603.
- (30) Briggs, L.; Hou, S.; Cui, C.; Fan, L. Simultaneous Type-I and Type-II Phase Matching for Second-Order Nonlinearity in Integrated Lithium Niobate Waveguide. *Opt. Express* **2021**, *29* (16), 26183.
- (31) Saleh, H. D.; Vezzoli, S.; Caspani, L.; Branny, A.; Kumar, S.; Gerardot, B. D.; Faccio, D. Towards Spontaneous Parametric down Conversion from Monolayer MoS₂. *Sci. Rep.* **2018**, *8* (1), 3862.
- (32) Okoth, C.; Cavanna, A.; Santiago-Cruz, T.; Chekhova, M. V. Microscale Generation of Entangled Photons without Momentum Conservation. *Phys. Rev. Lett.* **2019**, *123* (26), 263602.
- (33) Sultanov, V.; Santiago-Cruz, T.; Chekhova, M. V. Flat-Optics Generation of Broadband Photon Pairs with Tunable Polarization Entanglement. *Opt. Lett.* **2022**, *47* (15), 3872.
- (34) Guo, Q.; Qi, X.-Z.; Gao, M.; Hu, S.; Zhang, L.; Zhou, W.; Zang, W.; Zhao, X.; Wang, J.; Yan, B.; et al. Ultrathin Quantum Light Source with van der Waals NbOCl₂ crystal. *Nature* **2023**, *613*, 53–59.
- (35) Santiago-Cruz, T.; Fedotova, A.; Sultanov, V.; Weissflog, M. A.; Arslan, D.; Younesi, M.; Pertsch, T.; Staude, I.; Setzpfandt, F.;

- Chekhova, M. Photon Pairs from Resonant Metasurfaces. *Nano Lett.* **2021**, *21* (10), 4423–4429.
- (36) Parry, M.; Mazzanti, A.; Poddubny, A.; Valle, G. D.; Neshev, D. N.; Sukhorukov, A. A. Enhanced Generation of Nondegenerate Photon Pairs in Nonlinear Metasurfaces. *Adv. Photonics* **2021**, *3* (05), 1–6.
- (37) Zhang, J.; Ma, J.; Parry, M.; Cai, M.; Camacho-Morales, R.; Xu, L.; Neshev, D. N.; Sukhorukov, A. A. Spatially Entangled Photon Pairs from Lithium Niobate Nonlocal Metasurfaces. *Sci. Adv.* **2022**, *8* (30), 1–20.
- (38) Poddubny, A. N.; Neshev, D. N.; Sukhorukov, A. A. Quantum Nonlinear Metasurfaces. In *Nonlinear Meta-Optics*; CRC Press: 2020; pp 147–180.
- (39) Nikolaeva, A.; Frizyuk, K.; Olekhno, N.; Solntsev, A.; Petrov, M. Directional Emission of Down-Converted Photons from a Dielectric Nanoresonator. *Phys. Rev. A* **2021**, *103* (4), 43703.
- (40) Marino, G.; Solntsev, A. S.; Xu, L.; Gili, V. F.; Carletti, L.; Poddubny, A. N.; Rahmani, M.; Smirnova, D. A.; Chen, H.; Lemaître, A.; et al. Spontaneous Photon-Pair Generation from a Dielectric Nanoantenna. *Optica* **2019**, *6* (11), 1416.
- (41) Hanh Duong, N. M.; Saerens, G.; Timpu, F.; Buscaglia, M. T.; Buscaglia, V.; Morandi, A.; Muller, J. S.; Maeder, A.; Kaufmann, F.; Solntsev, A. S.; et al. Spontaneous Parametric Down-Conversion in Bottom-up Grown Lithium Niobate Microcubes. *Opt. Mater. Express* **2022**, *12* (9), 3696–3704.
- (42) Boyd, R. W. *Nonlinear Optics*; Elsevier Science: 2008; pp 1–67.
- (43) Papatryfonos, K.; Angelova, T.; Brimont, A.; Reid, B.; Guldin, S.; Smith, P. R.; Tang, M.; Li, K.; Seeds, A. J.; Liu, H.; et al. Refractive Indices of MBE-Grown $\text{Al}_x\text{Ga}(1-x)\text{As}$ Ternary Alloys in the Transparent Wavelength Region. *AIP Adv.* **2021**, *11* (2), 025327.
- (44) Dursap, T.; Vettori, M.; Danescu, A.; Botella, C.; Regreny, P.; Patriarche, G.; Gendry, M.; Penuelas, J. Crystal Phase Engineering of Self-Catalyzed GaAs Nanowires Using a RHEED Diagram. *Nanoscale Adv.* **2020**, *2* (5), 2127–2134.
- (45) Timofeeva, M.; Bouravleuv, A.; Cirlin, G.; Shtrom, I.; Soshnikov, I.; Reig Escalé, M.; Sergeyev, A.; Grange, R. Polar Second-Harmonic Imaging to Resolve Pure and Mixed Crystal Phases along GaAs Nanowires. *Nano Lett.* **2016**, *16* (10), 6290–6297.
- (46) Lenzini, F.; Poddubny, A. N.; Titchener, J.; Fisher, P.; Boes, A.; Kasture, S.; Haylock, B.; Villa, M.; Mitchell, A.; Solntsev, A. S.; et al. Direct Characterization of a Nonlinear Photonic Circuit's Wave Function with Laser Light. *Light Sci. Appl.* **2018**, *7* (1), 17143–17145.
- (47) Xiong, Q.; Chen, G.; Gutierrez, H. R.; Eklund, P. C. Raman Scattering Studies of Individual Polar Semiconducting Nanowires: Phonon Splitting and Antenna Effects. *Appl. Phys. A Mater. Sci. Process.* **2006**, *85* (3), 299–305.
- (48) Ren, M. L.; Liu, W.; Aspetti, C. O.; Sun, L.; Agarwal, R. Enhanced Second-Harmonic Generation from Metal-Integrated Semiconductor Nanowires via Highly Confined Whispering Gallery Modes. *Nat. Commun.* **2014**, *5*, 5432.
- (49) de Ceglia, D.; Carletti, L.; Galtarossa, A.; Vincenti, M. A.; de Angelis, C.; Scalora, M. Harmonic Generation in Mie-Resonant GaAs Nanowires. *Appl. Sci.* **2019**, *9*, 3381.
- (50) Yu, P.; Li, Z.; Wu, T.; Wang, Y. T.; Tong, X.; Li, C. F.; Wang, Z.; Wei, S. H.; Zhang, Y.; Liu, H.; et al. Nanowire Quantum Dot Surface Engineering for High Temperature Single Photon Emission. *ACS Nano* **2019**, *13* (11), 13492–13500.

□ Recommended by ACS

Two-Photon Excitation of Silicon-Vacancy Centers in Nanodiamonds for All-Optical Thermometry with a Noise Floor of $6.6 \text{ mK}\cdot\text{Hz}^{-1/2}$

Jiahua Zhang, Zhiqin Chu, et al.

JANUARY 30, 2023

THE JOURNAL OF PHYSICAL CHEMISTRY C

READ ▶

Gallium Phosphide Nanowires Grown on SiO_2 by Gas-Source Molecular Beam Epitaxy

Songdan Kang, Fariba Hatami, et al.

MARCH 10, 2023

CRYSTAL GROWTH & DESIGN

READ ▶

High-Performance Single-Photon Sources at Telecom Wavelength Based on Broadband Hybrid Circular Bragg Gratings

Andrea Barbiero, Andrew J. Shields, et al.

AUGUST 11, 2022

ACS PHOTONICS

READ ▶

Observation of Anomalous Negative Photoconductivity in Ga_2O_3 Nanowires: Implications for Broadening the Spectral Response of Photodetectors

Wei Ruan and Xianquan Meng

JANUARY 09, 2023

ACS APPLIED NANO MATERIALS

READ ▶

Get More Suggestions >